An Intersheet Packing Interaction in Aβ Fibrils Mapped by Disulfide Cross-Linking[†]

Shankaramma Shivaprasad and Ronald Wetzel*

Graduate School of Medicine, University of Tennessee, 1924 Alcoa Highway, Knoxville, Tennessee 37920

Received September 14, 2004; Revised Manuscript Received October 26, 2004

ABSTRACT: Most models for the central cross-β folding unit in amyloid fibrils of the Alzheimer's plaque protein Aβ align the peptides in register in H-bonded, parallel β-sheet structure. Some models require the Aβ peptide to undergo a chain reversal when folding into the amyloid core, while other models feature very long extended chains, or zigzag chains, traversing the protofilament. In this paper we introduce the use of disulfide bond cross-linking to probe the fold within the core and the packing interactions between β-sheets. In one approach, amyloid fibrils grown under reducing conditions from each of three double cysteine mutants (17/34, 17/35, and 17/36) of the Aβ(1−40) sequence were subjected to oxidizing conditions. Of these three mutants, only the Leu17Cys/Leu34Cys peptide could be cross-linked efficiently while resident in fibrils. In another approach, double Cys mutants were cross-linked as monomers before aggregation, and the resulting fibrils were assessed for stability, antibody binding, dye binding, and cross-seeding efficiency. Here too, fibrils from the 17/34 double Cys mutant most closely resemble wild-type Aβ(1−40) fibrils. These data support models of the Aβ fibril in which the Leu17 and Leu34 side chains of the same peptide pack against each other at the β-sheet interface within the amyloid core. Related cross-linking strategies may reveal longer range spatial relationships. The ability of the cross-linked 17/35 double Cys mutant Aβ to also make amyloid fibrils illustrates a remarkable plasticity of the amyloid structure and suggests a structural mechanism for the generation of conformational variants of amyloid.

Protein aggregation is a subject of intense research interest due to the association of protein misassembly with diseases such as Alzheimer's disease (AD)[1] and prion diseases (*1*). In many of these diseases, the principle aggregate seen at autopsy is the amyloid fibril (*2*). Although the main protein component of these aggregates differs from one disease to another, these amyloid fibrils share a number of structural properties, including long, unbranched, twisted fibrillar morphology, a "cross-β" X-ray diffraction pattern, and the ability to bind certain heteroaromatic dyes and conformational antibodies (*2*, *3*). While recent studies suggest that in some disease states other aggregated forms of the same proteins may be more central to the disease mechanism (*4*), mature amyloid fibrils almost certainly contribute to pathology in some diseases. Furthermore, structural characterization of fibrils may help to define the structures of other aggregated states, and tools developed for analysis of fibril structure may be helpful in characterizing other aggregates (*5*).

The most thoroughly studied amyloid fibrils are those derived from the amyloid β (Aβ) peptide associated with AD. Aβ fibrils exhibit the classic cross-β diffraction pattern, which is consistent with a β-sheet-rich structure in which extended chains are perpendicular to the fibril axis and backbone H-bonds run parallel to the axis (*6*). Although the Aβ peptides found in amyloid fibrils range up to about 43 amino acids long, the N-terminal 10−15 amino acids are not part of the β-sheet network of the fibril, since this portion of the peptide in fibrils is flexible (*7*), is accessible to limited proteolysis (*8*), and is insensitive to replacement by proline (*9*). The highly H-bonded amyloid core of Aβ fibrils, involving most of the residues in the 15−40 portion, has been shown to consist of Aβ molecules aligned in register in parallel β-sheets (*7*, *10*, *11*). Most models of how Aβ folds on itself within the protofilament substructure of the fibril (*9*, *11*, *12*) require the Aβ peptide to undergo some kind of chain reversal, so that N-terminal and C-terminal portions of the core sequence lie opposite each other across a sheet−sheet interface (see, for example, Figure 1). Yet to be established are the detailed orientations of these two sheets with respect to each other. Since the distances between α carbons in two packed sheets are longer (8−10 Å) than the distances separating the main chains of adjacent strands within a sheet (~5 Å), this aspect of fibril structure has been particularly challenging to address.

We have been applying a strategy combining site-directed mutagenesis and stability analysis to elucidate structural details of various Aβ aggregates. Recently, we identified potential turn locations within the amyloid core of Aβ fibrils using scanning proline mutagenic analysis (*9*) and used this information to help to guide the building of a working model for the Aβ protofilament (*12*) (Figure 1). Refinement of this

[†] This work was supported by NIH Grant 1 R01 AG18416 (to R.W.).

* To whom correspondence should be addressed: e-mail, rwetzel@mc.utmck.edu; phone, 865-544-9168; fax, 865-544-9235.

[1] Abbreviations: AD, Alzheimer's disease; Aβ, amyloid β protein (for sequence, see Materials and Methods); RP-HPLC, reverse-phase high-performance liquid chromatography; TFA, trifluoroacetic acid; ThT, thioflavin T; PBS, phosphate-buffered saline; PBSA, phosphate-buffered saline plus 0.05% (w/v) sodium azide; TCEP, tris(2-carboxyethyl)phosphine; EM, electron microscopy; LC/MS, liquid chromatography with mass spectroscopy.

10.1021/bi048019s CCC: $27.50
Published on Web 11/13/2004

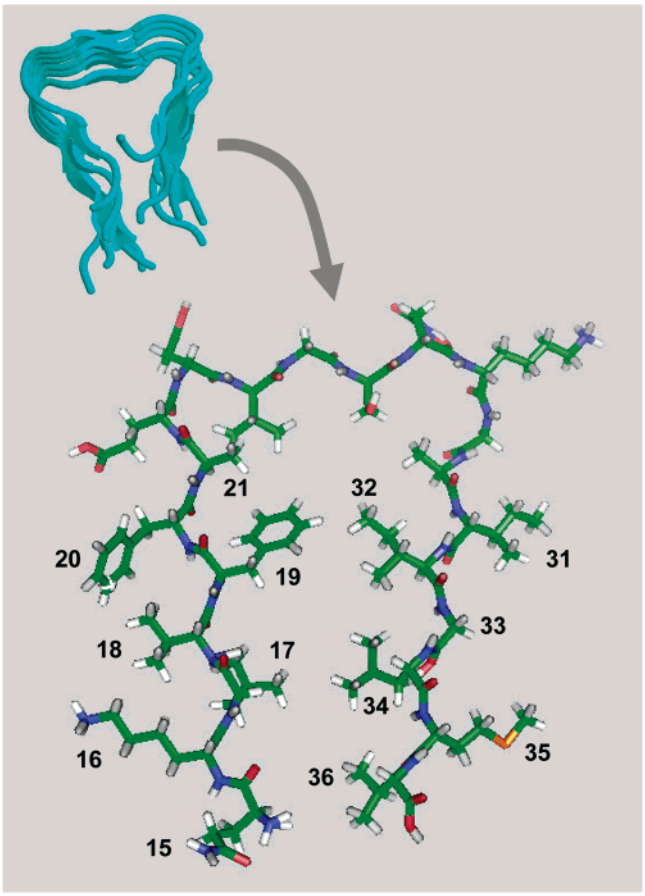

FIGURE 1: A model for a single strand of the 15−36 sequence of Aβ in the core, β-sheet portion of the amyloid fibril. The upper left cartoon shows a six-stranded model derived from proline scanning analysis (*9*) and protein threading (*12*). The lower right shows a single strand derived from this model, after adjustments (J. T. Guo and Y. Xu, unpublished results) based on single cysteine mutagenesis results (S. Shivaprasad and R. Wetzel, manuscript in preparation). Residue numbering: Asp of the sequence Asp-Ala-Glu-Phe is designated residue 1.

model requires additional data, including a knowledge of the orientations and spatial proximities of the amino acid side chains in the amyloid core region. We are using scanning cysteine and alanine mutagenesis to investigate side chain environments. Here, we describe the use of double Cys mutagenesis to probe the spatial proximity of specific pairs of amino acid side chains across the interface of the packed β-sheets in the Aβ fibril.

MATERIALS AND METHODS

All of the peptides used in this study were purchased from the Keck Biotechnology Center at Yale University. WT Aβ(1−40), having the sequence DAEFRHDSGYEVHHQKLVFFAEDVGSNKGAIIGLMVGGVV, was obtained as a pure peptide. Double cysteine replacement mutants of Aβ(1−40) were obtained unpurified. The crude peptides were purified on Bio-Rad RP-HPLC using a semipreparative C3 column and a water/acetonitrile gradient with 0.05% TFA. The identity and purity of the final peptides were confirmed by mass spectrometry and RP-HPLC on an Agilent 1100 series LC/MSD. All of the other chemicals used in this study were of reagent grade and were purchased from commercial sources. Quantitation of concentrations of monomeric Aβ was by analytical HPLC, by integration of the A_{220} peak and comparison to a standard curve from an Aβ(1−40) solution quantified by amino acid composition analysis (*8*). ThT fluorescence measurements were conducted as described (*13*,*14*) and the values adjusted for the weight of amyloid fibrils as indicated by HPLC analysis.

Intramolecular Disulfide Cross-Linking of Double Cys Peptides at the Monomer Level. Purified double cysteine mutant Aβ(1−40) peptides were incubated either in 0.1 M phosphate buffer (pH 8.0) or in 10% DMSO solution at room temperature and at a peptide concentration of 100 μM. The course of the reaction was monitored by reverse-phase HPLC, taking advantage of the HPLC mobility difference between cross-linked and non-cross-linked versions of the same sequence. Completion of the oxidation reaction was confirmed by the absence of sulfhydryl groups using Ellman's reagent (*15*). Peak identities including oxidation state were confirmed by mass spectroscopy. The rate of oxidation was faster in 10% DMSO than in 0.1 M phosphate buffer, but the products obtained from both reactions were identical.

Amyloid Fibril Assembly. Each double cysteine mutant was used to make fibrils under two sets of conditions. Under one set of conditions, the cysteine sufhydryls were oxidized before the fibril assembly reaction (see above) and incubated as described previously (*8*) to generate fibrils. Briefly, the disaggregated peptide was incubated at 37 °C in PBS (pH 7.5) containing 0.05% sodium azide (PBSA) together with a seed consisting of 0.1 wt % of sonicated wild-type Aβ-(1−40) fibrils. The progress of the reaction was monitored by ThT measurement of fibrils and by HPLC measurement of monomer.

Alternatively, the Cys sulfhydryls were kept in the reduced state during the course of fibril formation. In this case, we included 10 mM TCEP [tris(2-carboxyethyl) phosphine] (Pierce, Rockford, IL) and 1 mM EDTA in the PBSA buffer and bubbled argon gas through the buffer prior to dissolving Aβ, to keep the sulfhydryl side chain of cysteine in the reduced state during amyloid assembly. The assembly reactions were routinely carried out with a starting monomeric peptide concentration of about 50 μM and monitored by HPLC as described above. Fibrils collected from the assembly reaction by centrifugation were shown to contain only reduced peptide by HPLC analysis; as discussed below, inter- and intramolecular cross-linking alters the HPLC mobility of these peptides. Thus, isolated fibrils dissolved in formic acid and HPLC analyzed exhibited peak elution times and MS parent ions consistent with a reduced state. In a more stringent test, fibrils were treated with iodoacetic acid (10 mM, 20 min, room temperature, PBS) prior to dissolution with formic acid and HPLC analysis; only carboxamidomethyl-Cys forms of the Aβ(1−40) double Cys mutants were found, with near quantitative recovery of material, showing that fibrils grown from reduced Cys mutants under these conditions remain in the reduced state in the fibril.

As a noncovalent assembly, amyloid fibril formation in vitro is theoretically reversible and therefore should come to a thermodynamic equilibrium, an expectation confirmed by experiment (B. O'Nuallain and R. Wetzel, manuscript in preparation). Free energies describing fibril stability can be calculated from the corresponding equilibrium constants (*9*), which in the case of amyloid elongation are identical to the critical concentrations (C_rs) (*9*, *16*) obtained by HPLC measurement of the concentration of monomeric Aβ left in

solution at equilibrium. The difference between the ΔG values for mutant and wild-type Aβ is the $\Delta\Delta G$ describing the difference in free energies of dissociation between mutant and wild type, which under favorable circumstances (*9*) can be considered to be a measure of the destabilization of fibril structure by the mutation.

Oxidation of the Sulfhydryl Group at the Fibril Level. Proper analysis of the structure of Aβ within the fibrils requires excluding information from residual monomeric content. This is accomplished by (a) starting the oxidation reaction with fibrils free of monomer and (b) analyzing only the peptides derived from fibrils. Thus, reduced double Cys mutant fibrils were collected by centrifugation at 14800 rpm for 30 min at 4 °C. The supernatant was removed, the pellet suspended in 10% aqueous DMSO in PBS to a final concentration of 0.45 mg/mL, and the mixture incubated at room temperature. To monitor oxidation, aliquots were removed and ultracentrifuged at 85000 rpm (315000*g*) at 4 °C for 30 min, and the supernatant was carefully removed. The fibril pellet was then dissolved in 5% formic acid and analyzed by LC/MS; material recovery by HPLC analysis was consistently greater than 80%. To confirm that the analysis really indicates the cross-linked state of the peptide resident within the fibrils, a control experiment was run in which the fibril pellet after oxidation was resuspended and treated with iodoacetic acid before dissolution and analysis. This treatment, which quantitatively yields alkylated Cys products when run on fibrils containing Cys residues in the reduced state (see above), yielded distributions of cross-linked and non-cross-linked peptides identical to those obtained from analyses performed without a prior alkylation step.

Antibody Binding. The antibody used in this study is a monoclonal IgM, WO1, generated against Aβ fibrils and capable of recognizing a number of different amyloid fibrils (*3*). High-binding microtiter plates (Costar) were coated with 100 ng/well of sonicated aggregate and blocked with 1% BSA in PBSA. A dilution series of WO1 was added, and the plates were incubated for 1 h at 37 °C and then washed. The amount of WO1 bound was detected using a 1:5000 (v/v) dilution of biotinylated goat anti-mouse antibody (Sigma), and the biotin was quantified using a 1:1000 (v/v) dilution of the europium−streptavidin complex, with europium quantified on a Victor^2 time-resolved fluorescence microtiter plate reader (both reagent and instrument were from Perkin-Elmer Wallac).

Microplate Elongation Assay. As described previously (*17*), fibrils were immobilized onto microtiter plate wells, the plates were incubated various times with 10 nM biotinyl-Aβ(1−40) and then washed, and the signal was developed with europium-tagged streptavidin followed by time-resolved fluorescence as described above. The rates of the initial, fast phase are reported.

Electron Microscopy. The fibrils grown in PBSA were adsorbed onto carbon and formavar-coated copper grids and negatively stained with 0.5% (w/v) uranyl acetate solution. The stained grids after washing of the excess uranyl acetate were examined and photographed on a Hitachi-600 electron microscope.

RESULTS

The structural model for the Aβ(1−40) protofilament shown in Figure 1 was generated by a combination of experiment (*9*) and computational analysis (*12*). In this model, the H-bonded core of the prismatic protofilament is composed of a stack of parallel-aligned Aβ 15−36 segments, with the backbone H-bonds of the three β-sheet faces of the prism running parallel to the protofilament axis and the side chains of amino acids in the β-sheet portions projecting into or out of the core. The two hydrophobic segments of Aβ with high β-sheet potential, LVFFA and IIGLMV, are on opposite long faces of the prism. In a similar model based on solid-state NMR data, these two sequence elements are also involved in adjacent β-sheets (*11*). In both models, the exact orientations of the sheets to each other are poorly defined because of a lack of data on (a) which side chains within these segments are thrust into the core and which are pointing out from the core and (b) how the two adjacent sheets are aligned with each other, with respect to the interaction of internalized side chains.

Side chain accessibility experiments using single Cys mutants of Aβ(1−40) (S. Shivaprasad and R. Wetzel, manuscript in preparation) suggest that residue 17 is directed into the packed core, as shown in Figure 1. We therefore picked the residue 17 side chain as a probe to identify its packing partner(s) projecting from the opposite face of the protofilament prism within the amyloid core (see Figure 1). On the basis of the rough model shown in Figure 1, three double Cys mutants of Aβ(1−40) were prepared: L17C/L34C, L17C/M35C, and L17C/V36C. These were purified by HPLC and their structures confirmed by mass spectrometry. As described below, these mutants were used in several different ways to probe the internal β-sheet packing within the amyloid core.

Oxidative Cross-Linking of Reduced Peptides within Amyloid Fibrils. Each of the double Cys mutants was incubated under standard conditions with added reducing agent (Materials and Methods). To encourage these mutant peptides to grow into amyloid fibrils resembling wild-type Aβ fibrils, we seeded some reactions with 0.1 wt % WT Aβ(1−40) fibrils (*18*), while parallel reactions were conducted without seeds. In the seeded reactions, we observed roughly similar fibril formation rates for all three double Cys mutants, as monitored by ThT fluorescence, with lag times in the range of 5−6 days (Figure 2a). In contrast, WT Aβ-(1−40) seeded with WT fibrils typically gives a lag time of 1−2 days (Figure 2b). In these experiments, the double Cys mutants exhibited similar lag times with and without seeding with 0.1% wild-type fibrils; it is likely that higher seeding levels would have reduced the lag time of fibril growth for these mutants, but this was not attempted. The aggregated products from the double Cys mutants are amyloid fibrils, as judged by EM analysis (Figure 3), anti-amyloid antibody binding (Table 1), Congo red birefringence (not shown), and hydrogen−deuterium exchange analysis (*19*) (not shown). Although the weight-normalized ThT fluorescence yields of these fibrils are significantly lower than that of WT fibrils (Table 1), it is not unusual to observe substantial variations in ThT fluorescence yields of fibrils from Aβ mutants (A. Williams, S. Shivaprasad, and R. Wetzel, unpublished observations).

Critical concentrations (C_rs) were determined for amyloid formation from reduced double Cys mutants using HPLC on centrifugation supernatants. We used the C_r values to calculate the ΔG values for fibril stabilization under these

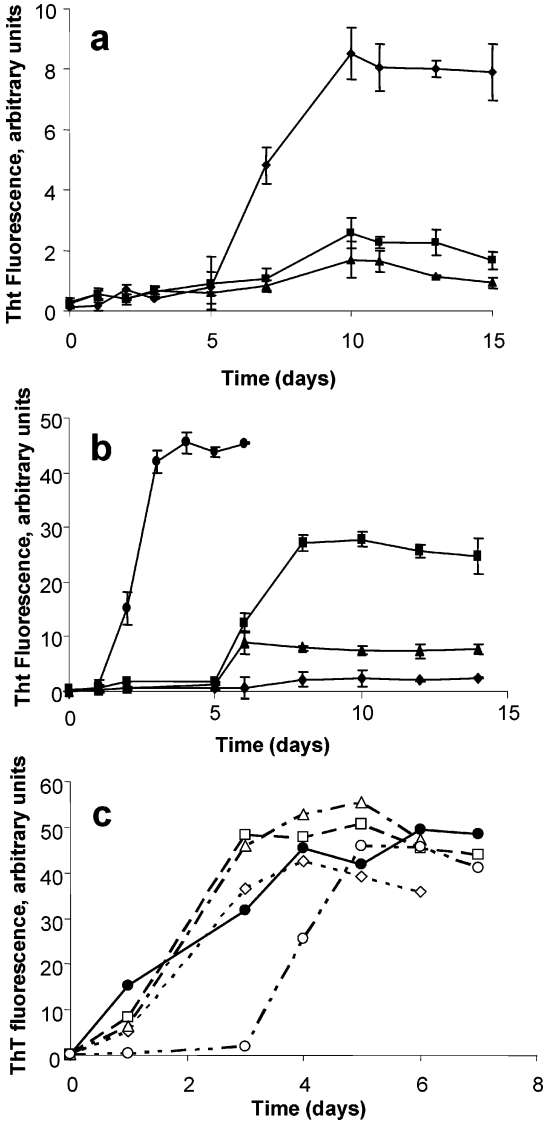

FIGURE 2: Seeded amyloid formation by various forms of Aβ(1−40). Reactions were constructed with disaggregated Aβ monomers, seeded with 0.1% (a and b) or 1% (c) by weight fibrils, and monitored by taking aliquots and determining relative fibril levels by the ThT method (Materials and Methods). (a) Reduced double Cys mutants seeded with WT fibrils. (b) Oxidized double Cys mutants seeded with WT fibrils. (c) WT monomeric Aβ(1−40) seeded with fibrils grown from oxidized double Cys mutants or WT (control). Key: wild-type monomers seeded with WT fibrils (●); wild-type monomers, unseeded (○); 17/34 mutant (■ or □); 17/35 mutant (◆ or ◇); 17/36 mutant (▲ or △).

buffer conditions (Materials and Methods) (*9*). We found that the ΔG values for all three reduced double Cys mutants are significantly higher than for wild-type fibrils, indicating destabilization of fibril structure by the Cys replacements (Figure 4). The destabilization of Aβ fibrils by these reduced double Cys mutations is of the same order of magnitude (1.5−2.5 kcal/mol) as a Pro substitution at position Ile[31] or Ile[32] (*9*), reflecting a significant degree of structural incompatibility of the reduced Cys side chains within the Aβ fold in the fibrils.

These fibrils were subjected to oxidation in 10% DMSO at room temperature and analyzed at various times for any cross-linking within the fibril (Materials and Methods). Under the conditions studied, only fibrils made from the reduced L17C/L34C mutant gave efficient disulfide cross-linking of

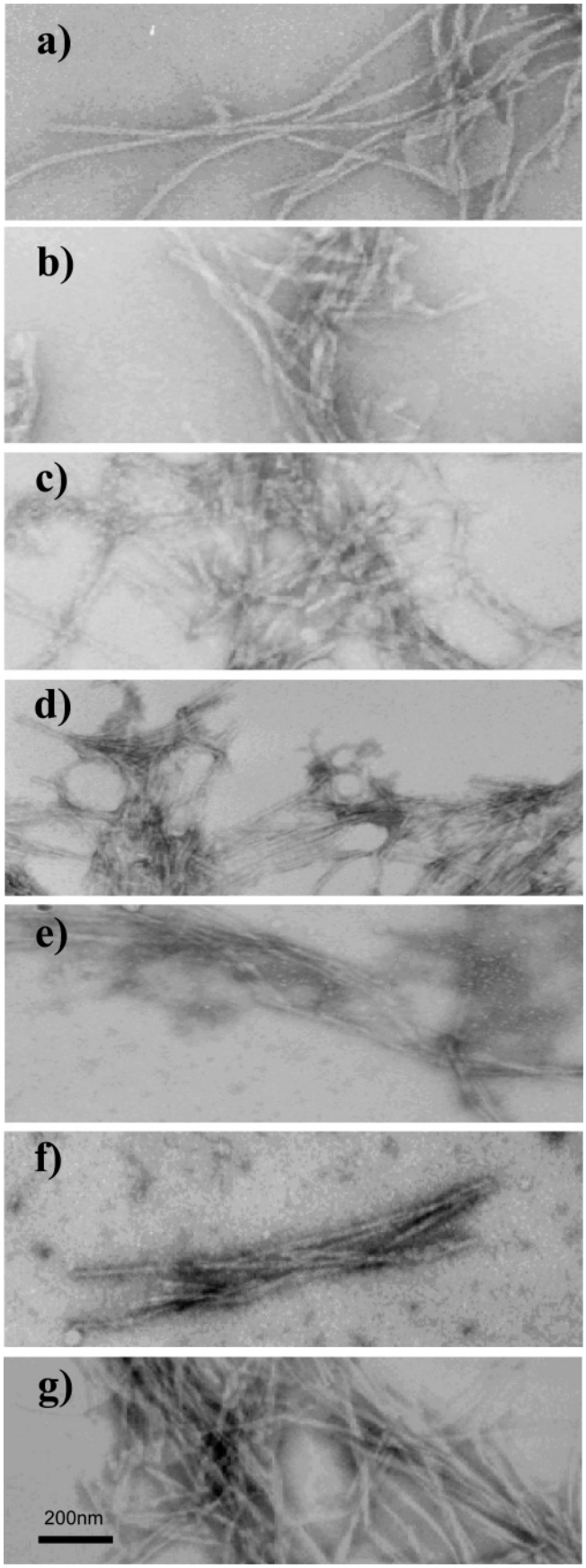

FIGURE 3: Electron micrographs of amyloid fibrils made from wild-type and double Cys mutant Aβ(1−40) peptides. (a) Reduced L17C/L34C. (b) Reduced L17C/M35C. (c) Reduced L17C/V36C. (d) Oxidized L17C/L34C. (e) Oxidized L17C/M35C. (f) Oxidized L17C/V36C. (g) WT Aβ(1−40). Magnification = 50000×; scale bar = 200 nm.

Table 1: Amyloid Properties of Aβ(1−40) Amyloid Fibrils

	EC_{50} values for WO1 (nM)[a]		ThT fluorescence (arbitrary units)[b]		elongation rate (fmol/min)[c]
	reduced	oxidized	reduced	oxidized	oxidized
WT[d]	6.3 ± 1	6.3 ± 1	50 ± 4	50 ± 4	0.119
L17C/L34C	20 ± 4	13 ± 1	5.4 ± 0.7	25 ± 1	0.141
L17C/M35C	32 ± 3	32 ± 1	10.3 ± 1.3	3.0 ± 0.7	0.092
L17C/V36C	79 ± 4	25 ± 4	1.8 ± 0.2	8.0 ± 2	0.107

[a] EC_{50} values are the concentrations at which binding is half of the maximal binding in the microtiter plate antibody binding assay described in Materials and Methods. [b] Values for an aliquot of a fibril suspension were analyzed and then adjusted for the weight of fibrils present in the suspension, as determined by HPLC (see Materials and Methods). [c] Elongation rates from the fast phase of a microplate elongation assay (*17*) in which different WT Aβ(1−40) amyloid fibrils are used as seeds. These WT Aβ fibrils were produced from a WT monomer when seeded with fibrils of either wild-type Aβ(1−40) or oxidized double Cys mutants (Figure 2c). [d] All data in this row are from normal WT fibrils that have not been exposed to either reducing or oxidizing conditions; column heads refer to treatment of double Cys mutants as described in Materials and Methods.

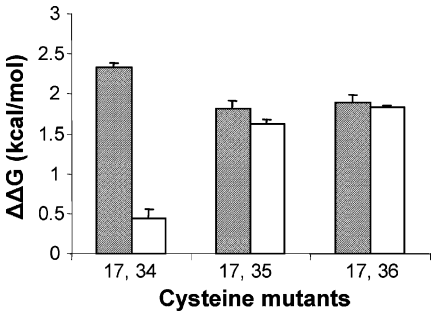

FIGURE 4: Effect of cysteine mutations on fibril stability. $\Delta\Delta G$ values for the difference in stability between mutant and wild type are shown for each double Cys mutant. Positive values reflect destabilization with respect to wild-type Aβ(1−40) fibrils; by definition, the $\Delta\Delta G$ for wild type is zero. The shaded bars correspond to the reduced mutants, and the open bars correspond to the oxidized mutants.

any kind on oxidation; LC/MS analysis of the dissolved fibril oxidation product from L17C/L34C Aβ(1−40) shows complete conversion to the corresponding intramolecularly cross-linked peptide (Figure 5). In contrast, the L17C/V36C mutant gave a poor yield of intramolecularly cross-linked peptide as the only product, but only after an extended incubation time (1 week), suggesting that a significant energy barrier must be overcome in order for the Cys residues of the L17C/V36C fibrils to become oriented for favorable cross-linking. Finally, the L17C/M35C fibrils showed no measurable formation of an intramolecular disulfide bond. On prolonged oxidation, the only oxidation product at all is a small amount of dimeric peptide formed by disulfide cross-linking between Cys residues of two monomers (Figure 5). It is likely that this dimer arises from oxidation of the Cys^{35} residues of two monomers, but this has to be confirmed. Thus, these results confirm that the side chain of residue 17 is pointing into the amyloid core and suggest that this side chain packs against the side chain of residue 34 from the same peptide molecule as it projects into the core from the opposed β-sheet. The results also suggest that residues 34 and 36 are both inward facing, while residue 35 is outward facing (relative orientations that are, of course, expected for a sequence of contiguous residues in β-sheet).

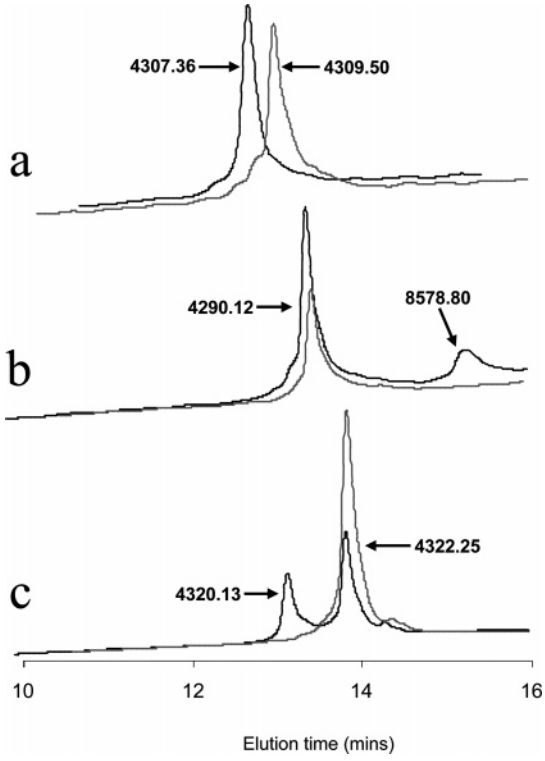

FIGURE 5: HPLC profile monitoring the effect of oxidation (in 10% DMSO) of fibrils composed of reduced double Cys Aβ(1−40) mutants. The *y* axis is the peptide bond absorbance at 218 nm. Peaks are labeled with parent ion molecular weights derived from on-line electrospray MS analysis. Note the difference of 2 Da between oxidized and reduced mutants; in panel b, MWs correspond to reduced monomer (4290.12) and disulfide-linked dimer (8578.80). (a) L17C/34C, 0 h (gray line) and 24 h (black line). (b) L17C/M35C, 0 h (gray line) and 84 h (black line). (c) L17C/V36C, 0 h (gray line) and 192 h (black line).

Fibril Formation by Cross-Linked Monomeric Double Cys Mutants. The three monomeric double Cys mutant peptides were also subjected to oxidative cross-linking as described (Materials and Methods). All three peptides could be converted to the intramolecularly cross-linked form; products were confirmed to be cyclic disulfides by their decreased mass (2 Da from loss of hydrogens during sulfydryl oxidation) and their faster elution time in HPLC. Interestingly, the relative reaction rates for intramolecular cross-linking differed appreciably between the three peptides, in the order L17C/L34C ≫ L17C/M35C ∼ L17C/V36C (data not shown). The same relative rates are obtained regardless of which method of oxidation is used. These results suggest the existence of conformational preferences within the monomer population under these conditions, a result consistent with recent NMR analysis of Aβ monomers in native buffer (*20*).

These cross-linked monomers were purified by HPLC and incubated under standard fibril growth conditions, seeded with 0.1 wt % of Aβ(1−40) fibrils. All three peptides showed good fibril growth under these conditions (Figure 2b). Interestingly, all three mutants exhibit lag times of about 5 days, significantly longer than that of WT monomer; higher seeding levels might well have reduced these lag times. Furthermore, like the reduced peptides (see above), the oxidized peptides produce fibrils that give standard ThT responses but with different weight-normalized ThT fluorescence yields, as seen with other Aβ mutants (A. Williams

and R. Wetzel, unpublished results). The significance of the similarities in fibril formation kinetics among the three cross-linked Aβ mutants is not clear. Although relative rates of heterologous seeding of fibril elongation by related sequences may contain information about fibril structure (*17*), the experiments here were not designed to explore such differences but rather were simply designed to produce fibrils for analysis. In addition to their ThT response, the aggregates produced are typical amyloid fibrils by both EM (Figure 3) and anti-amyloid antibody analysis (Table 1).

Monomer concentrations at equilibrium (C_r) were determined (Materials and Methods) and converted to ΔG values (Materials and Methods). These data (Figure 4) show several interesting effects. First, the only amyloid fibril with a stability comparable to WT Aβ(1−40) is the oxidized L17C/L34C peptide. This double Cys mutant is also unique in that fibrils made from the cross-linked form are significantly more stable than fibrils made from the corresponding reduced form, corresponding to a $\Delta\Delta G$ of 1.89 kcal/mol in stabilization energy, suggesting that the disulfide bond between residues 17 and 34 is particularly compatible with the amyloid structure. In contrast, the amyloid fibrils from the other two double Cys mutants are significantly less stable than wild-type fibrils, whether oxidized or reduced, so that in these cases cross-linking does not provide any significant additional stability. Since the degree of stabilization of a folded protein provided by introduction of a disulfide bond generally depends on a balance of subtle stabilizing and destabilizing effects (*21*, *22*), it is not possible at present to specify how the net stabilization of the cross-linked 17/34 mutant is achieved or to analyze these data in more detail.

Given the surprising ability of cross-linked 17/35 Aβ to make amyloid fibrils that in many ways resemble WT fibrils, we explored the relative abilities of the fibrils produced from oxidized monomers to act as seeds for elongation of wild-type Aβ(1−40). Seeded elongation assays can serve as sensitive indicators of the structural relatedness of fibrils (*17*). Figure 2c summarizes a solution phase assay that shows that WT Aβ(1−40) monomer aggregates with very similar kinetics when seeded with either WT fibrils or fibrils of any of the three cross-linked double Cys mutants. Interesting, fibrils made from the cross-linked 17/35 mutant seed WT elongation essentially as efficiently as WT fibrils.

The ability of all three cross-linked Aβ peptides to make amyloid fibrils capable of seeding elongation by WT Aβ-(1−40) monomer suggests a possible structural mechanism for the generation of different conformational states of fibrils. Thus, while cross-linked 17/34 makes fibrils that are WT-like, cross-linked 17/35 requires a 180° rotation of the extended chain in order to form the opposing β-sheet, and cross-linked 17/36 forces a change in register across the sheet interface. If these three amyloid fibrils indeed adopt different conformations, one might expect the fibrils to display different properties expected from conformational variants. For example, they might exhibit different efficiencies of seeding fibril formation by WT Aβ(1−40), and the fibrils thus formed might in turn retain conformational differences evidenced by their seeding propensities. However, the growth kinetics and ThT fluorescence yields for WT Aβ(1−40) fibrils generated by seeding with the cross-linked mutants appear identical (Figure 2c). Furthermore, when these progeny fibrils are immobilized onto plastic and used as seeds for elongation by additional WT Aβ(1−40), an assay that can be quite sensitive to fibril structure (*17*), the initial elongation rates of all three are similar and roughly comparable to normal WT fibrils as seeds (Table 1). Thus, there is no strong evidence for conformational differences between the cross-linked 17/34, 17/35, and 17/36 fibrils, even though these fibrils must in fact differ significantly in the nature of their β-sheet arrangements.

Antibody Binding Studies. We analyzed the fibrils for their affinities and binding amplitudes for the pan-amyloid monoclonal antibody WO1. This antibody recognizes, with different selectivities, amyloid fibrils from many different proteins, while not reacting with the monomeric precursor proteins (*3*). The results (Table 1) show that the mutant fibrils exhibit significant differences from WT fibrils in WO1 binding. The amyloid fibrils from the oxidized 17/34 mutant exhibit an apparent binding constant only 2-fold weaker than that of WT fibrils, while the other oxidized mutant fibrils are 4−5-fold weaker than WT. Interestingly, binding strength of WO1 to the mutant fibrils is better by a factor of 2−3 comparing oxidized and reduced peptides of all three double Cys mutants, suggesting that a more rigid structure may improve or help to solidify the epitope.

Thioflavin T Fluorescence. Like Congo red, thioflavin T binding, with concomitant change in fluorescence properties, is a common feature of many amyloid fibrils (*13*, *14*). The weight-normalized ThT values (see Materials and Methods) for the WT and the six possible double Cys mutant Aβ fibrils are shown in Table 1. Clearly, the oxidized 17/34 fibrils are most like WT in their ThT response.

DISCUSSION

Distance restraints obtained to date for Aβ fibrils (*7*, *10*, *11*) are adequate for making approximate intermolecular alignments between H-bonded strands within a single β-sheet of the fibril (typically about 5 Å), but determination of through-space contacts between residues in adjacent, packed sheets (typically 8−10 Å) is much more challenging because of the greater distance. Since Aβ peptides in the amyloid fibril appear to be aligned in register in parallel β-sheets in the H-bonded core region, and since the β-strands of the core region are broken by one or more turns (*7*, *9*, *11*), the most likely [but not the only possible (*23*)] protofilament topology features packing between β-sheets comprising the N- and C-terminal segments within the core sequence of the same molecule (Figure 1). Data presented here support such models, showing that Aβ peptides containing a covalent cross-link between these two segments within the same peptide can make amyloid fibrils that very closely resemble the fibrils generated from wild-type Aβ(1−40). Furthermore, our data consistently point to the most likely structure being one in which the side chains of residues 17 and 34 are in close contact in the packed hydrophobic core of the fibril. The cross-linking data render much less likely models involving Aβ peptides that do not contain a significant chain reversal within the Aβ peptide.

We consider the definitive evidence in favor of the 17−34 interaction to be the data from oxidative cross-linking of fibrils containing reduced double Cys mutant Aβ peptides. These data clearly show that Cys residues at positions 17 and 34 are particularly well positioned to make an intramo-

lecular disulfide while the peptide is locked within the fibril. The 17/35 and 17/36 mutants show that the facile cross-linking seen in the 17/34 mutant is not typical of other double Cys mutants. The inability of 17/35 to make any cross-linked monomer within the fibril context contrasts with the ability of the monomeric peptide to be cross-linked in solution. One obvious possible constraint on reactivity in the fibril would be if the Cys^{35} side chain were rigidly oriented, pointing out from the protofilament, as shown in Figure 1. This orientation is also suggested by Cys accessibility experiments (S. Shivaprasad and R. Wetzel, manuscript in preparation). Finally, the 17/36 mutant is able to be cross-linked within the fibril, but only at a very slow rate. A model consistent with all of these data would be one related to Figure 1 but in which the chain segments are slightly offset against each other so that the residue 17 side chain is between the residue 34 and 36 side chains emerging from the opposing strand.

Considering that the structural models (*9*, *11*, *12*) consist of parallel strands of Aβ in register, it is interesting that, in the oxidation of reduced fibrils, none of the double Cys mutants exhibit any trace of intermolecular disulfide formation between equivalent residues in adjacent Aβ molecules. The absence of such dimers presumably reflects structural constraints within the fibril. In fact, disulfide bonding between neighboring residues in adjacent strands of a β-sheet is very rare, due to steric constraints (*24*).

It should be noted that, in general, cross-linking between noncontiguous elements of a peptide while resident in an amyloid fibril is not absolute proof of their physical proximity within the packed fibril. Any relatively long-lived reactive species can become involved in cross-links if it has the flexibility to migrate within the structure and seek out reaction partners. In the case of the data presented here, several pieces of evidence suggest that the Cys residues in these mutants are not in regions of the flexible polypeptide chain and that most are not solvent exposed. First, in independent experiments, single Cys Aβ mutants at positions 17, 34, and 36 are all completely protected from alkylation when the peptide is incorporated into amyloid, under conditions where Cys mutations in the mobile N-terminus are alkylated (S. Shivaprasad and R. Wetzel, unpublished results); this suggests that these residues are in rigid, protected environments. While Cys at position 35 can be alkylated in the fibril state (S. Shivaprasad and R. Wetzel, unpublished results), it is probably not mobile, given the rigidity of the flanking 34 and 36 residues. Second, the absence of multiple products including symmetric and asymmetric disulfide dimers suggests a restricted reactivity most consistent with geometrically constrained environments for the Cys residues at these positions.

Although interpretation of the cross-linking data is straightforward and seems firm, it is gratifying that thermodynamic stability analysis confirms that the 17−34 cross-link seems more compatible with the Aβ(1−40) fibril structure than the other two cross-links. Figure 4 shows that the $\Delta\Delta G$ for the oxidized 17/34 mutant is very close to that for WT Aβ while the $\Delta\Delta G$ values for the other double Cys mutants, oxidized or reduced, indicate significantly less stable fibrils. Furthermore, Figure 4 shows that oxidation does not improve fibril stability for the 17/35 or 17/36 mutants, while significantly improving the stability of the 17/34 mutant.

Other data from measurements diagnostic of amyloid fibrils show that the cross-linked 17/34 mutant makes amyloid fibrils highly similar to WT Aβ(1−40) fibrils. For example, the conformational anti-amyloid antibody WO1 (*3*) binds to all the aggregates reported here, but 17−34 cross-linked fibrils yield a binding constant most like that of WT fibrils (Table 1). Table 1 also shows that the ThT fluorescence yield of cross-linked 17/34 fibrils is only a factor of 2 different from that of WT fibrils, while the cross-linked 17/35 and 17/36 fibrils exhibit much more significantly reduced values compared to WT fibrils, as do amyloid fibrils from all three reduced double Cys mutants. The significance of the ThT results is difficult to gauge, since the basis of mutational effects on ThT fluorescent yields is not known.

One surprising feature of these results is the ability of all three cross-linked monomers to make typical amyloid fibrils. Although the 17/34 cross-linked form of Aβ appears most compatible with WT fibril structure, the other two disulfide mutants also make good fibrils. It is especially striking that the 17/35 cross-linked peptide makes fibrils, since to do so must involve rotation of the 31−36 extended chain element by 180°, altering the inward and outward facing residues in this segment. Fibrils from all three cross-linked monomers, nonetheless, are capable of seeding elongation by the WT Aβ(1−40) monomer (Figure 2c) and exhibiting other features of amyloid (Table 1). These observations point to the resiliency of the amyloid structure, previously indicated by the response of Aβ to proline mutations (*9*). Similar results were apparently obtained in attempts to use disulfide cross-linking to identify a presumptive β-turn in the Aβ amyloid structure (*25*). The ability to form amyloid fibrils from sequences that force significant changes in local structure within the fibril is consistent with, and may help to explain, the apparent ability of one polypeptide sequence to grow into the multiple conformations of amyloid fibril responsible for some prion strain phenomena (*26*). At the same time, we found no evidence for differences in seeding abilities of the fibrils from the three cross-linked variants.

On an important practical note, the ability of each of these double Cys mutants to make fibrils suggests that it will not be sufficient to simply confirm amyloid formation when assessing the results of mutagenesis and cross-linking experiments. Data on the structural relatedness of mutant and WT fibrils is required before the relevance of the mutant fibrils can be determined.

Disulfide bonds are occasionally found between two packed β-sheets in a folded protein, for example in the core of the immunoglobulin fold β-sandwich/β-barrel (*24*). While the $C_\alpha-C_\alpha$ distance range of disulfide bonds in protein structures, 4.6−7.4 Å, is on the low side of the typical 8−10 Å range for sheet−sheet separations in proteins, the 7.4 Å value from an immunoglobulin β-sandwich (*24*) shows that disulfide bonds can indeed span two β-sheets, as required here for formation of amyloid structure. Furthermore, disulfide bonds have also been observed across the β-helix interior in a small parallel β-helical antifreeze protein (*27*), which may possibly be a better model for the packed β-structure within the amyloid fibril (*28*). Disulfide-bonded proteins, such as insulin, are known to be capable of making amyloid fibrils, and this additional structural restraint offers both challenges and opportunities in model building of amyloid structure from such molecules (*29*). This pilot study of three

double Cys mutants of Aβ(1−40) clearly demonstrates the feasibility of the method as well as an important distance restraint in fibril structure. Analysis of additional double Cys mutants, based on our evolving model of the Aβ amyloid fibril, should provide more structural details on the Aβ fibril and possibly other aggregated states of Aβ as well. In particular, structural relationships between protofilaments in the fibril, which will be especially challenging to measure, may be amenable to cross-linking analysis using oxidation as well as bifunctional cross-linking reagents. In addition, it is of great interest to evaluate the structure of the Aβ protofibril, a species recently implicated as the main toxic form of Aβ in Alzheimer's disease, and how it might relate to amyloid fibril structure (*5*).

ACKNOWLEDGMENT

We thank Jun-tao Guo and Ying Xu for the figures showing the Aβ fibril model.

REFERENCES

1. Martin, J. B. (1999) Molecular basis of the neurodegenerative disorders, *N. Engl. J. Med. 340*, 1970−1980 [erratum: (1999) *N. Engl. J. Med. 341*, 1407].
2. Sipe, J. D., and Cohen, A. S. (2000) Review: history of the amyloid fibril, *J. Struct. Biol. 130*, 88−98.
3. O'Nuallain, B., and Wetzel, R. (2002) Conformational antibodies recognizing a generic amyloid fibril epitope, *Proc. Natl. Acad. Sci. U.S.A. 99*, 1485−1490.
4. Caughey, B., and Lansbury, P. T. (2003) Protofibrils, pores, fibrils, and neurodegeneration: separating the responsible protein aggregates from the innocent bystanders, *Annu. Rev. Neurosci. 26*, 267−298.
5. Kheterpal, I., Lashuel, H. A., Hartley, D. M., Walz, T., Lansbury, P. T., Jr., and Wetzel, R. (2003) Abeta protofibrils possess a stable core structure resistant to hydrogen exchange, *Biochemistry 42*, 14092−14098.
6. Sunde, M., and Blake, C. (1997) The structure of amyloid fibrils by electron microscopy and X-ray diffraction, *Adv. Protein Chem. 50*, 123−159.
7. Torok, M., Milton, S., Kayed, R., Wu, P., McIntire, T., Glabe, C. G., and Langen, R. (2002) Structural and dynamic features of Alzheimer's abeta peptide in amyloid fibrils studied by site-directed spin labeling, *J. Biol. Chem. 277*, 40810−40815.
8. Kheterpal, I., Williams, A., Murphy, C., Bledsoe, B., and Wetzel, R. (2001) Structural features of the Aβ amyloid fibril elucidated by limited proteolysis, *Biochemistry 40*, 11757−11767.
9. Williams, A. D., Portelius, E., Kheterpal, I., Guo, J. T., Cook, K. D., Xu, Y., and Wetzel, R. (2004) Mapping abeta amyloid fibril secondary structure using scanning proline mutagenesis, *J. Mol. Biol. 335*, 833−842.
10. Benzinger, T. L., Gregory, D. M., Burkoth, T. S., Miller-Auer, H., Lynn, D. G., Botto, R. E., and Meredith, S. C. (1998) Propagating structure of Alzheimer's beta-amyloid(10−35) is parallel beta-sheet with residues in exact register, *Proc. Natl. Acad. Sci. U.S.A. 95*, 13407−13412.
11. Petkova, A. T., Ishii, Y., Balbach, J. J., Antzutkin, O. N., Leapman, R. D., Delaglio, F., and Tycko, R. (2002) A structural model for Alzheimer's beta-amyloid fibrils based on experimental constraints from solid-state NMR, *Proc. Natl. Acad. Sci. U.S.A. 99*, 16742−16747.
12. Guo, J.-T., Wetzel, R., and Xu, Y. (2004) Molecular modeling of the core of Aβ amyloid fibrils, *Proteins 57*, 357−364.
13. Naiki, H., Higuchi, K., Hosokawa, M., and Takeda, T. (1989) Fluorometric determination of amyloid fibrils in vitro using the fluorscent dye, thioflavine T, *Anal. Biochem. 177*, 244−249.
14. LeVine, H. (1999) Quantification of β-sheet amyloid fibril structures with thioflavin T, *Methods Enzymol. 309*, 274−284.
15. Means, G. E., and Feeney, R. E. (1971) *Chemical Modification of Proteins*, Holden-Day, San Francisco.
16. Harper, J. D., and Lansbury, P. T., Jr. (1997) Models of amyloid seeding in Alzheimer's disease and scrapie: mechanistic truths and physiological consequences of the time-dependent solubility of amyloid proteins, *Annu. Rev. Biochem. 66*, 385−407.
17. O'Nuallain, B., Williams, A. D., Westermark, P., and Wetzel, R. (2004) Seeding specificity in amyloid growth induced by heterologous fibrils, *J. Biol. Chem. 279*, 17490−17499.
18. Wood, S. J., Chan, W., and Wetzel, R. (1996) Seeding of Aβ fibril formation is inhibited by all three isotypes of apolipoprotein E, *Biochemistry 35*, 12623−12628.
19. Kheterpal, I., Zhou, S., Cook, K. D., and Wetzel, R. B. (2000) A-beta amyloid fibrils possess a core structure highly resistant to hydrogen exchange, *Proc. Natl. Acad. Sci. U.S.A. 97*, 13597−13601.
20. Hou, L., Shao, H., Zhang, Y., Li, H., Menon, N. K., Neuhaus, E. B., Brewer, J. M., Byeon, I. J., Ray, D. G., Vitek, M. P., Iwashita, T., Makula, R. A., Przybyla, A. B., and Zagorski, M. G. (2004) Solution NMR studies of the A beta(1−40) and A beta(1−42) peptides establish that the Met35 oxidation state affects the mechanism of amyloid formation, *J. Am. Chem. Soc. 126*, 1992−2005.
21. Wetzel, R. (1987) Harnessing disulfide bonds using protein engineering, *Trends Biochem. Sci. 12*, 478−482.
22. Betz, S. F. (1993) Disulfide bonds and the stability of globular proteins, *Protein Sci. 2*, 1551−1558.
23. Kajava, A. V., Baxa, U., Wickner, R. B., and Steven, A. C. (2004) A model for Ure2p prion filaments and other amyloids: the parallel superpleated beta-structure, *Proc. Natl. Acad. Sci. U.S.A. 101*, 7885−7890.
24. Thornton, J. M. (1981) Disulphide bridges in globular proteins, *J. Mol. Biol. 151*, 261−287.
25. Hilbich, C., Kisters, W. B., Reed, J., Masters, C. L., and Beyreuther, K. (1991) Aggregation and secondary structure of synthetic amyloid beta A4 peptides of Alzheimer's disease, *J. Mol. Biol. 218*, 149−163.
26. Tanaka, M., Chien, P., Naber, N., Cooke, R., and Weissman, J. S. (2004) Conformational variations in an infectious protein determine prion strain differences, *Nature 428*, 323−328.
27. Liou, Y. C., Tocilj, A., Davies, P. L., and Jia, Z. (2000) Mimicry of ice structure by surface hydroxyls and water of a beta-helix antifreeze protein, *Nature 406*, 322−324.
28. Wetzel, R. (2002) Ideas of order for amyloid fibril structure, *Structure 10*, 1031−1036.
29. Jimenez, J. L., Nettleton, E. J., Bouchard, M., Robinson, C. V., Dobson, C. M., and Saibil, H. R. (2002) The protofilament structure of insulin amyloid fibrils, *Proc. Natl. Acad. Sci. U.S.A. 99*, 9196−9201.

BI048019S